IEEE Access
Multidisciplinary | Rapid Review | Open Access Journal

Received March 2, 2020, accepted March 19, 2020, date of publication March 30, 2020, date of current version April 16, 2020.

Digital Object Identifier 10.1109/ACCESS.2020.2984314

Balun LNA Thermal Noise Analysis and Balancing With Common-Source Degeneration Resistor

QUSAI M. ABUBAKER AND LUTFI ALBASHA, (Senior Member, IEEE)
Electrical Engineering Department, American University of Sharjah, Sharjah 26666, UAE

Corresponding author: Qusai M. Abubaker (b00061510@aus.edu)

This work was supported in part by the Open Access Program from the American University of Sharjah.

ABSTRACT The Balun low noise amplifier (LNA) is an LNA that exploits a combination of a common-source (CS) and a common-gate (CG) transistors, which cancels the noise and distortion of the CG stage. And since the CG is known to be linear, only the CS needs to be carefully designed and optimized. The Balun LNA also cancels the distortion and noise of the CG. In this paper, the CS section will be fully analyzed, and shown how the condition set in the literature review still satisfy the balancing output and cancel the CS stage thermal noise as well as the CG thermal noise. Also, forward body biasing (FBB) is used to reduce the threshold voltage and an addition of CS degeneration resistor to balance the output while still canceling the thermal noise of the transistors is tested using UMC180nm on Cadence. The LNA achieves a gain of 19-16dB, NF $<$ 3.6 over the bandwidth 200M-1.9GHz without a CS degeneration. A 17.8-14.8dB gain, a NF $<$ 3.8 over the bandwidth 200MHz-2.1GHz and power consumption of 12mW in both cases. Although outside the bandwidth, at ISM 2.4GHz a gain of 14.5dB and a NF of 3.8 is achieved, making it suitable for wireless sensor node (WSN) applications. According to the author's knowledge, this is the first time the degeneration resistor noise analysis on a Balun LNA is derived and analyzed.

INDEX TERMS Low-noise amplifiers, thermal noise, noise figure, circuit analysis.

I. INTRODUCTION

The CS LNA possesses better NF and more gain than the CG LNA at low frequencies at the cost of power or off chip components. Increasing the frequency of operation requires more stable circuit elements, such as the CG. This means that expanding the analysis on how to improve the noise figure (NF) of CG was necessary for wideband and high frequencies operations. This paper will take the CS thermal noise of the Balun LNA fully into consideration with and without a CS degeneration resistor. A new set of condition to balance and cancel the thermal noise will also be derived and presented. Another technique used was FBB to reduce the Vth of the LNA. A real device study was conducted using UMC180nm technology on cadence virtuoso, with one component using the cadence Analog library; reason will be explained.

II. LITRETURE REVIEW

The Balun LNA is a single input to double ended output. Most Balun applications did not change the properties (such as size) of the transistors, which made it appear unbalanced. In [1] the Balun was thoroughly discussed, canceling the CG thermal noise and distortion and giving a set of equation to ensure the LNA is balanced. In [2] a CG LNA was designed using cross coupling capacitors, while improving the NF. In [3] an all MOSFET Balun LNA was made with a simplified NF, in [4]the design and measurement of a balance wideband LNA was presented. In [5] Differential Balun LNA was used with BiCMOS, where the CE-stage acts as the error correction stage canceling distortion and noise, although he used degeneration resistors for both CE, there noise contribution was not fully derived nor was the CE noise contribution studied. In [6] four different Balun LNA topologies were explained and studied, deriving a new tunable bandpass topology; again no noise contribution from the CS or the CS degeneration resistor was accounted for. In [7] a Balun LNA was used with a CG stage before the Balun itself for matching purposes, but no CS degeneration resistor was added. In [8] Balun LNA was used, with cascaded structure on the CG, but no new noise figure was derived and no CS degeneration was used. In [9] instead of a global negative feedback technique which helps in improving NF and matching at the price of stability, a feedforward noise-canceling technique was used allowing for noise and impedance matching, while canceling the distortion and noise of the matching amplifiers. In [10] a

The associate editor coordinating the review of this manuscript and approving it for publication was Dušan Grujić.

resistive feedback was used to increase the bandwidth, the NF was improved by adding a gm-enhanced cascaded amplifiers with a source follower feedback. In [11] a Balun LNA and a wide tuning range synthesizer is used to cover major frequency bands of use today, the design does include a mixer and a programmable integration sampler and clock discrete-time filters, although the emphasis of the measurement where the LNA, no new noise figure or degeneration source where used. In [12] an ESD-protected Balun LNA with an inductorless broadband input matching is offered, the amplification stage exploited double current reuse and a single-stage thermal noise cancellation to enhance the gain, NF and power consumption. In [13] a Balun LNA using g''_m compensation technique at the output to improve the limited gain of the CG stage. The Balun LNA is working in parallel with two g''_m compensation transistors; one for every output stage; improving the gain by 5.4-5.8 dB, this technique also improved the linearity performance. In [14] an inductorless Balun LNA for low power multiband and multi-standard radios is proposed, the LNA uses dual shunt feedback to reduce the bias current needed by the CG while this current is reused in the CS stage, the NF is derived but for the whole system not just the Balun LNA. In [15] a new modified current-bleeding (CBLD) technique was used to cancel the noise of the Balun LNA, this method helps solve the issue of balancing the Balun with different resistors causing phase mismatch due to different RC constant. A comparison between the conventional and modified CBLD technique is tested, the modified CBLD uses an extra resistor at the drain of the MOSFET in the CBLD circuit, this increases the input impedance seen by the source of the CBLD circuit (due to channel length modulation), therefore reducing the overall noise, unfortunately, the Balun NF derived is a cascaded structure Balun and not useful for this papers analysis. In this paper, a complete noise analysis will be derived, where part of the noise equation in equation (1) [1] will be shown. The condition set for output balancing will be tested and verified by the noise analysis in this paper.

In the differential pair, the noise of each transistor is referred to the input and then multiplied by the gain of the other transistor. The total output noise of the single transistor in a differential pair is the output noise the first transistor produces, added to the input referred noise of the second transistor multiplied by the gain of first.

The noise figure (NF) of the Balun LNA will only consider the thermal noise of the transistors, resistors, and the source. Moreover, the circuit is considered to have an infinite output impedance, and ideal bias sources.

The NF in [1] is:

$$F = 1 + \frac{\gamma g_{mCG}\left(R_{CG} - R_S g_{mCS} R_{CS}\right)^2}{R_s A_V^2} + \frac{\gamma g_{mCS} R_{CS}^2 \left(1 + g_{mCG} R_S\right)^2}{R_s A_V^2} + \frac{\left(R_{CG} + R_{CS}\right)\left(1 + g_{mCG} R_S\right)^2}{R_s A_V^2} \quad (1)$$

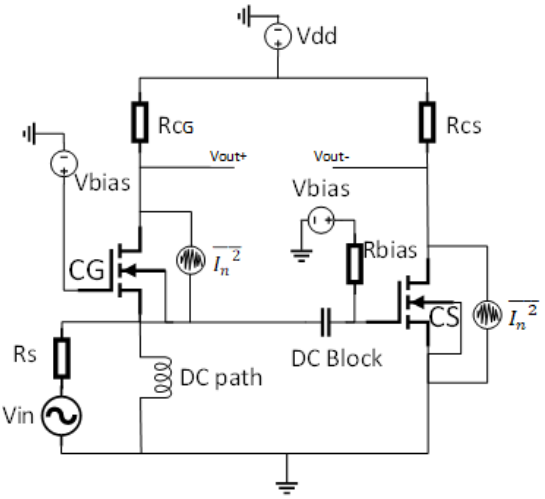

FIGURE 1. Balun LNA, a combination of CS and CG.

where A_v is the total gain of the Balun LNA taken to be $A_v = g_{mCG}R_{CG} + g_{mCS}R_{CS}$, were g_{mCS} and g_{mCG} are the transconductance of the CS and CG respectively. R_{CS} and R_{CG} are the drain resistance of CS and CG respectively, R_s is the source resistance, and finally γ the noise coefficient (=2/3 in long channel). The first term in (1) is the noise of the source, second is the CG, third is the CS, and fourth is the resistors. But it doesn't take the CS input referred noise into consideration.

In [3] the NF of the Balun was found to be:

$$NF = 1 + \frac{k_f}{8kTR_S g_m^2 c_{ox} f^{\alpha f}}\left(\frac{g_{m1}^2}{W_1 L_1} + \frac{g_m^2}{W_2 L_2}\right) + \frac{\gamma}{2R_S g_m} + \frac{1}{R_S R_D g_m} \quad (2)$$

The first term is the source noise, second is flicker, third is transistor thermal noise and fourth is the resistor thermal noise. Where $g_{m1} = g_{mCG}$, $g_{mb1} = g_{mbCG}$ (the body effect of the CG), $g_{m2} = g_{mCS}$, W is the width and L is the length. The conditions applied in (2) were:

$$\begin{aligned} g_m &= g_{m2} = (g_{m1} + g_{mb1}) \\ L_1 &= L_2 \\ r_{o1} &= r_{o2} = r_o \\ r_{o1}(g_{m1} + g_{mb1}) &\gg 1 \\ I_{DCG} &= I_{DCS} \\ R_{CG} &= R_{CS} = R \\ \boldsymbol{A_{vLNA}} &= \boldsymbol{\frac{2r_o R_D g_m}{r_o + R_D}} \end{aligned}$$

III. NOISE ANALYSIS

Two noise equations were presented above in (1) and (2), the following steps are a third noise analysis based on equation (1) method. Focusing on the second and third terms of equation (1), which represent thermal noise, in [16] a step by step analysis follows.

The gain of the CG is given by [17]:

$$A_{vCG} = g_{mCG}R_{CG} \tag{3}$$

The gain of the CS is given by [17]:

$$A_{vCS} = -g_{mCS}R_{CS} \tag{4}$$

The gain of the LNA is the difference between CG and CS gains:

$$A_{vLNA} = g_{mCG}R_{CG} + g_{mCS}R_{CS} \tag{5}$$

The voltage noise of the CG:

$$\overline{Vout_{CG}} = \overline{I_{nCG}}R_{CG} \tag{6}$$

CG noise referred to the input:

$$\overline{Vin_{CG}} = \frac{\overline{I_{nCG}}R_{CG}}{|A_{vCG}|} = \frac{\overline{I_{nCG}}}{g_{mCG}} \tag{7}$$

The output voltage noise of the CS:

$$\overline{Vout_{CS}} = \overline{I_{nCS}}R_{CS} \tag{8}$$

The CS noise referred to the input:

$$\overline{Vin_{CS}} = \frac{\overline{I_{nCS}}R_{CS}}{|A_{vCS}|} = \frac{\overline{I_{nCS}}}{g_{mCS}} \tag{9}$$

Total output noise of the CG when considering the input referred noise of the CS is (using the above equations):

$$\overline{Vout_{CG,total}} = \overline{I_{nCG}}R_{CG} + \frac{\overline{I_{nCS}}}{g_{mCS}} * g_{mCG}R_{CG} \tag{10}$$

The total output voltage noise of the CS when considering the input referred voltage noise of the CG is also given by:

$$\overline{Vout_{CS,total}} = \overline{I_{nCS}}R_{CS} + \frac{\overline{I_{nCG}}}{g_{mCG}} * g_{mCS}R_{CS} \tag{11}$$

The voltage noise of the source is:

$$\overline{V_{ns}} = \overline{V_n} * \left(\frac{R_{in}}{R_{in} + R_s}\right) \tag{12}$$

And $\overline{V_n^2}$ is the power of the noise given to be [17]:

$$\overline{V_n^2} = 4KTR_S \tag{13}$$

Assuming, $R_{in} = \frac{1}{g_{mCG}}$, which is the low frequency matching condition of the CG

Therefore,

$$\overline{V_{ns}} = \overline{V_n} * \left(\frac{1}{1 + g_{mCG}R_S}\right) \tag{14}$$

where K is Boltzmann constant, T is temperature in kelvin and R is the source resistance

Total voltage noise of the LNA:

$$\overline{Vout_{LNA}} = \overline{Vout_{CG,total}} - \overline{Vout_{CS,total}} \tag{15}$$

Dividing by noise of the source resistance:

$$\frac{\overline{Vout_{LNA}}}{\overline{V_{ns}}} = \left(\overline{Vout_{CG,total}} - \overline{Vout_{CS,total}}\right) * \frac{1 + g_{mCG}R_S}{\overline{V_n}} \tag{16}$$

Substituting the proper terms and simplifying:

($\overline{V_n}$ *was moved to the left side to ease calculation*):

$$\begin{aligned}\frac{\overline{Vout_{LNA}}}{\overline{V_{ns}}} * \overline{V_n} &= \left(\begin{array}{l}\overline{I_{nCG}}R_{CG} + \frac{\overline{I_{nCS}}}{g_{mCS}} * g_{mCG}R_{CG} + \overline{I_{nCG}}R_{CG}g_{mCG}R_s \\ \quad + \frac{\overline{I_{nCS}}}{g_{mCS}} * g_{mCG}R_{CG}g_{mCG}R_s\end{array}\right) \\ &\quad - \left[\begin{array}{l}\overline{I_{nCS}}R_{CS} + \frac{\overline{I_{nCG}}}{g_{mCG}} * g_{mCS}R_{CS} + \overline{I_{nCS}}R_{CS}g_{mCG}R_s \\ \quad + \frac{\overline{I_{nCG}}}{g_{mCG}} * g_{mCS}R_{CS}g_{mCG}R_s\end{array}\right]\end{aligned} \tag{17}$$

Grouping terms containing $\overline{I_{nCG}}$:

$$\begin{aligned}&\overline{I_{nCG}}R_{CG} + \overline{I_{nCG}}R_{CG}g_{mCG}R_s - \frac{\overline{I_{nCG}}}{g_{mCG}} * g_{mCS}R_{CS} \\ &\qquad - \frac{\overline{I_{nCG}}}{g_{mCG}}g_{mCS}R_{CS}g_{mCG}R_s\end{aligned} \tag{18}$$

Grouping terms containing $\overline{I_{nCG}}$ into two terms:

$$\overline{I_{nCG}}\left(R_{CG} - \frac{1}{g_{mCG}} * g_{mCS}R_{CS}g_{mCG}R_s\right) \tag{19}$$

$$= \overline{I_{nCG}}\left(R_{CG} - R_{CS}g_{mCS}R_s\right)$$

$$\overline{I_{nCG}}\left(R_{CG}g_{mCG}R_s - \frac{\overline{1}}{g_{mCG}} * g_{mCS}R_{CS}\right) \tag{20}$$

Grouping terms containing $\overline{I_{nCS}}$:

$$\begin{aligned}&\frac{\overline{I_{nCS}}}{g_{mCS}} * g_{mCG}R_{CG} + \frac{\overline{I_{nCS}}}{g_{mCS}} * g_{mCG}R_{CG}g_{mCG}R_s - \overline{I_{nCS}}R_{CS} \\ &\quad - \overline{I_{nCS}}R_{CS}g_{mCG}R_s \\ &= \overline{I_{nCS}}\left(\frac{1}{g_{mCS}} * g_{mCG}R_{CG} + \frac{1}{g_{mCS}} * g_{mCG}R_{CG}g_{mCG}R_s\right. \\ &\quad \left. - R_{CS} - R_{CS}g_{mCG}R_s\right)\end{aligned} \tag{21}$$

After grouping the noise terms with their respective noise currents, next step is to add them back and square to get the noise power:

$$\begin{aligned}&\frac{\overline{Vout_{LNA}^2}}{\overline{V_{ns}^2}} * \overline{V_n^2} \\ &= \overline{I_{nCG}^2}\left(R_{CG} - R_{CS}g_{mCS}R_s\right)^2 \\ &\quad + \overline{I_{nCG}^2}\left(R_{CG}g_{mCG}R_s - \frac{\overline{1}}{g_{mCG}} * g_{mCS}R_{CS}\right)^2 \\ &\quad + \overline{I_{nCG}^2}\left|\left(R_{CG} - R_{CS}g_{mCS}R_s\right)\left(R_{CG}g_{mCG}R_s\right.\right.\end{aligned}$$

$$-\frac{\overline{I}}{g_{mCG}} * g_{mCS}R_{CS}\Bigg)\Bigg| + \overline{I_{nCS}^2}\left(\frac{1}{g_{mCS}} * g_{mCG}R_{CG} + \frac{1}{g_{mCS}} * g_{mCG}R_{CG}g_{mCG}R_s - R_{CS} - R_{CS}g_{mCG}R_s\right)^2 \tag{22}$$

Finally, dividing by the gain of the LNA squared to refer the noise to the input (23) as as shown at the bottom of this page, The total NF is:

$$F = 1 + \overline{Vin_{LNA}^2} + \frac{(R_{CG} + R_{CS})\,(1 + g_{mCG}R_S)^2}{R_s A_V^2} \tag{24}$$

The reason for grouping the terms containing $\overline{I_{nCG}}$ into two terms is to show the second term from (1) is in (23) as the first term. Three more terms appear in (23) that do not in (1).

IV. BALANCING CONDITIONS

The Balun design condition set in [1] to achieve the best NF and balanced output are as follows:

$$g_{mCS} = n g_{mCG} \tag{25}$$

$$R_{CS} = \frac{R_{CG}}{n} \tag{26}$$

$$R_S = \frac{1}{g_{mCG}} \tag{27}$$

When these conditions where set in (23), a complete cancelation of thermal noise and output balancing is achieved. In other words, the differential pair thermal noise is canceled, making use of the differential pair noise property.

Substituting the conditions set in [1]; (25), (26), (27); into (23).

First Term:

$$\frac{\gamma g_{mCG}\,(R_{CG} - R_{CS}g_{mCS}R_s)^2}{R_s * A_{vLNA}^2} = \frac{\gamma g_{mCG}\left(R_{CG} - \frac{R_{CG}}{n} n g_{mCG}\frac{1}{g_{mCG}}\right)^2}{R_s * A_{vLNA}^2} = 0$$

Second Term:

$$\frac{\gamma g_{mCG}\left(R_{CG}g_{mCG}R_s - \frac{\overline{I}}{g_{mCG}} * g_{mCS}R_{CS}\right)^2}{R_s * A_{vLNA}^2} = \frac{\gamma g_{mCG}\left(R_{CG}g_{mCG}\frac{1}{g_{mCG}} - \frac{\overline{I}}{g_{mCG}} * n g_{mCG}\frac{R_{CG}}{n}\right)^2}{R_s * A_{vLNA}^2} = 0$$

Third Term and Fourth Term as shown at the bottom of the next page.

V. BALANCING WITH CS DEGENERATION

Balun balancing with a degeneration source on the CS stage was not done before, a complete analysis will be derived in this section and simulated in the following section. If the unbalance is produced due to the CS having higher gain than the CG, balancing with a degeneration resistor is possible. Ignoring the set condition in [1], it is possible to increase the linearity of the system and cancel the transistors thermal noise. Adding a degeneration resistor does increase the flexibility of the system and adds one more degree of freedom to the design. Detailed analysis follows:

Balancing the LNA with R_{SCS}

The gain of the CG is still as in equation (3).

The gain of the CS is given by [17]:

$$A_{vCS} = -\frac{g_{mCS}R_{CS}}{1 + g_{mCS}R_{SCS}} \tag{28}$$

The voltage noise of the CG is still as (6).

CG noise referred to the input is still as (7).

The output voltage noise of the CS is still as (8).

The CS noise referred to the input:

$$\overline{Vin_{CS}} = \frac{\overline{I_{nCS}}R_{CS}}{|A_{vCS}|} = \frac{\overline{I_{nCS}}\,(1 + g_{mCS}R_{SCS})}{g_{mCS}} \tag{29}$$

Total output noise of the CG when considering the input referred noise of the CS is (using the above equations):

$$\overline{Vout_{CG,total}} = \overline{I_{nCG}}R_{CG} + \frac{\overline{I_{nCS}}\,(1 + g_{mCS}R_{SCS})}{g_{mCS}} * g_{mCG}R_{CG} \tag{30}$$

$$\overline{Vin_{LNA}^2} = \frac{\gamma g_{mCG}\,(R_{CG} - R_{CS}g_{mCS}R_s)^2}{R_s * A_{vLNA}^2} + \frac{\gamma g_{mCG}\left(R_{CG}g_{mCG}R_s - \frac{\overline{I}}{g_{mCG}} * g_{mCS}R_{CS}\right)^2}{R_s * A_{vLNA}^2} + \frac{\gamma g_{mCG}\left|(R_{CG} - R_{CS}g_{mCS}R_s)\left(R_{CG}g_{mCG}R_s - \frac{\overline{I}}{g_{mCG}} * g_{mCS}R_{CS}\right)\right|}{R_s * A_{vLNA}^2} + \frac{\gamma g_{mCS}\left(\frac{1}{g_{mCS}} * g_{mCG}R_{CG} + \frac{1}{g_{mCS}} * g_{mCG}R_{CG}g_{mCG}R_s - R_{CS} - R_{CS}g_{mCG}R_s\right)^2}{R_s * A_{vLNA}^2} \tag{23}$$

The total output voltage noise of the CS when considering the input referred voltage noise of the CG is also given by:

$$\overline{Vout_{CS,total}} = \overline{I_{nCS}}R_{CS} + \frac{\overline{I_{nCG}}}{g_{mCG}} * \frac{g_{mCS}R_{CS}}{1 + g_{mCS}R_{SCS}} \quad (31)$$

Total voltage noise of the LNA:

$$\overline{Vout_{LNA}} = \overline{Vout_{CG,total}} - \overline{Vout_{CS,total}}$$

Dividing by noise of the source resistance:

$$\frac{\overline{Vout_{LNA}}}{\overline{V_{ns}}} = \left(\overline{Vout_{CG,total}} - \overline{Vout_{CS,total}}\right) * \frac{1 + g_{mCG}R_S}{\overline{V_n}}$$

Substituting the proper terms and simplifying:

($\overline{V_n}$ *moved to the left side to simplify calculation*):

$$\begin{aligned}
&\frac{\overline{Vout_{LNA}}}{\overline{V_{ns}}} * \overline{V_n} \\
&= \left[\overline{I_{nCG}}R_{CG} + \frac{\overline{I_{nCS}}\,(1 + g_{mCS}R_{SCS})}{g_{mCS}} * g_{mCG}R_{CG}\right. \\
&\quad + \overline{I_{nCG}}R_{CG}g_{mCG}R_s + \frac{\overline{I_{nCS}}\,(1 + g_{mCS}R_{SCS})}{g_{mCS}} \\
&\quad \left. * g_{mCG}R_{CG}g_{mCG}R_s\right] \\
&\quad - \left[\begin{array}{c} \overline{I_{nCS}}R_{CS} + \dfrac{\overline{I_{nCG}}}{g_{mCG}} * \dfrac{g_{mCS}R_{CS}}{1 + g_{mCS}R_{SCS}} \\ + \overline{I_{nCS}}R_{CS}g_{mCG}R_s + \dfrac{\overline{I_{nCG}}}{g_{mCG}} * \dfrac{g_{mCS}R_{CS}g_{mCG}R_s}{1 + g_{mCS}R_{SCS}} \end{array}\right]
\end{aligned} \quad (32)$$

Grouping $\overline{I_{nCG}}$ and $\overline{I_{nCS}}$ from (32), (33), (34) as shown at the bottom of the next page.

After grouping the noise terms with their respective noise currents, next step is to add them back and square to get the noise power:

$$\begin{aligned}
&\frac{\overline{Vout_{LNA}^2}}{\overline{V_{ns}^2}} * \overline{V_n^2} \\
&= \overline{I_{nCG}^2}\left[R_{CG} + R_{CG}g_{mCG}R_s - \frac{1}{g_{mCG}} * \frac{g_{mCS}R_{CS}}{1 + g_{mCS}R_{SCS}}\right. \\
&\quad \left. - \frac{g_{mCS}R_{CS}R_s}{1 + g_{mCS}R_{SCS}}\right]^2 \\
&\quad + \overline{I_{nCS}^2}\left[\frac{1 + g_{mCS}R_{SCS}}{g_{mCS}} * g_{mCG}R_{CG} + \frac{(1 + g_{mCS}R_{SCS})}{g_{mCS}}\right. \\
&\quad \left. * g_{mCG}^2R_{CG}R_s - R_{CS} - R_{CS}g_{mCG}R_s\right]^2
\end{aligned} \quad (35)$$

An R_{scs} is to be picked to cancel the thermal noise.

$$R_{scs} = \frac{g_{mCS}R_{CS} - g_{mCG}R_{CG}}{g_{mCS}g_{mCG}R_{CG}} \quad (36)$$

The R_{scs} equation is also the same equation found if $A_{vCG} = |A_{vCS}|$ and solving for R_{scs}:

$$g_{mCG}R_{CG} = \frac{g_{mCS}R_{CS}}{1 + g_{mCS}R_{SCS}}$$

Substituting (37) into (34):

$$\begin{aligned}
&\overline{I_{nCG}}[R_{CG} + R_{CG}g_{mCG}R_s - \frac{1}{g_{mCG}} \\
&\quad * \frac{g_{mCS}R_{CS}}{1 + g_{mCS}\frac{g_{mCS}R_{CS} - g_{mCG}R_{CG}}{g_{mCS}g_{mCG}R_{CG}}} \\
&\quad - \frac{g_{mCS}R_{CS}R_s}{1 + g_{mCS}\frac{g_{mCS}R_{CS} - g_{mCG}R_{CG}}{g_{mCS}g_{mCG}R_{CG}}}] \\
&= \overline{I_{nCG}}[R_{CG} + R_{CG}g_{mCG}R_s - \frac{g_{mCS}R_{CS}}{g_{mCG} + \frac{g_{mCS}R_{CS} - g_{mCG}R_{CG}}{R_{CG}}} \\
&\quad - \frac{g_{mCS}R_{CS}R_s}{1 + \frac{g_{mCS}R_{CS} - g_{mCG}R_{CG}}{g_{mCG}R_{CG}}}] \\
&= \overline{I_{nCG}}\left[R_{CG} + R_{CG}g_{mCG}R_s\right. \\
&\quad \left. - \frac{g_{mCS}R_{CS}R_{CG}}{g_{mCG}R_{CG} + g_{mCS}R_{CS} - g_{mCG}R_{CG}}\right. \\
&\quad \left. - \frac{g_{mCS}R_{CS}R_sg_{mCG}R_{CG}}{g_{mCG}R_{CG} + g_{mCS}R_{CS} - g_{mCG}R_{CG}}\right] \\
&= \overline{I_{nCG}}\left[R_{CG} + R_{CG}g_{mCG}R_s\right. \\
&\quad \left. - \frac{g_{mCS}R_{CS}R_{CG}}{g_{mCS}R_{CS}} - \frac{g_{mCS}R_{CS}R_sg_{mCG}R_{CG}}{g_{mCS}R_{CS}}\right] \\
&= \overline{I_{nCG}}\left[R_{CG} + R_{CG}g_{mCG}R_s - R_{CG} - R_{CG}g_{mCG}R_s\right] \\
&= 0
\end{aligned}$$

$$\frac{\gamma g_{mCG}\left|(R_{CG} - R_{CS}g_{mCS}R_s)\left(R_{CG}g_{mCG}R_s - \frac{\overline{1}}{g_{mCG}} * g_{mCS}R_{CS}\right)\right|}{R_s * A_{vLNA}^2}$$

$$= \frac{\gamma g_{mCG}\left|\left(R_{CG} - \frac{R_{CG}}{n}ng_{mCG}\frac{1}{g_{mCG}}\right)\left(R_{CG}g_{mCG}\frac{1}{g_{mCG}} - \frac{\overline{1}}{g_{mCG}} * ng_{mCG}\frac{R_{CG}}{n}\right)\right|}{R_s * A_{vLNA}^2} = 0$$

$$\frac{\gamma g_{mCS}\left(\frac{1}{g_{mCS}} * g_{mCG}R_{CG} + \frac{g_{mCG}R_{CG}g_{mCG}R_s}{g_{mCS}} - R_{CS} - R_{CS}g_{mCG}R_s\right)^2}{R_s * A_{vLNA}^2}$$

$$= \frac{\gamma g_{mCS}\left(\frac{g_{mCG}R_{CG}}{ng_{mCG}} + \frac{1}{ng_{mCG}} * g_{mCG}R_{CG}g_{mCG}\frac{1}{g_{mCG}} - \frac{R_{CG}}{n} - \frac{R_{CG}}{n}g_{mCG}\frac{1}{g_{mCG}}\right)^2}{R_s * A_{vLNA}^2} = 0$$

Substituting (35) into (33):

$$\begin{aligned}
&\overline{I_{nCS}}\left[\frac{1+g_{mCS}\frac{g_{mCS}R_{CS}-g_{mCG}R_{CG}}{g_{mCS}g_{mCG}R_{CG}}}{g_{mCS}} * g_{mCG}R_{CG}\right.\\
&\quad+\frac{\left(1+g_{mCS}\frac{g_{mCS}R_{CS}-g_{mCG}R_{CG}}{g_{mCS}g_{mCG}R_{CG}}\right)}{g_{mCS}} * g_{mCG}^2R_{CG}R_s - R_{CS}\\
&\quad\left.-R_{CS}g_{mCG}R_s\right]\\
&=\overline{I_{nCS}}\left[\frac{1+\frac{g_{mCS}R_{CS}-g_{mCG}R_{CG}}{g_{mCG}R_{CG}}}{g_{mCS}} * g_{mCG}R_{CG}\right.\\
&\quad+\frac{\left(1+\frac{g_{mCS}R_{CS}-g_{mCG}R_{CG}}{g_{mCG}R_{CG}}\right)}{g_{mCS}} * g_{mCG}^2R_{CG}R_s - R_{CS}\\
&\quad\left.-R_{CS}g_{mCG}R_s\right]\\
&=\overline{I_{nCS}}\left[\frac{g_{mCG}R_{CG}+g_{mCS}R_{CS}-g_{mCG}R_{CG}}{g_{mCS}}\right.\\
&\quad* +\frac{\left(g_{mCG}^2R_{CG}R_s+g_{mCS}R_{CS}g_{mCG}R_s-g_{mCG}^2R_{CG}R_s\right)}{g_{mCS}}\\
&\quad\left.-R_{CS}-R_{CS}g_{mCG}R_s\right]\\
&=\overline{I_{nCS}}\left[R_{CS} * +R_{CS}g_{mCG}R_s-R_{CS}-R_{CS}g_{mCG}R_s\right]\\
&=0
\end{aligned}$$

Finally, dividing by the gain of the LNA squared to refer the noise to the input (37), as shown at the bottom of the next page.

The total NF of the LNA with R_{SCS} is:

$$NF=1+\frac{\overline{Vin_{LNA}^2}}{}+\frac{(R_{CG}+R_{CS})\,(1+g_{mCG}R_S)^2}{R_sA_V^2}+\frac{R_{SCS}}{R_s} \quad (38)$$

VI. SIMULATION RESULTS

Using United Microelectronics Corporation (UMC180nm) process design kit (PDK) in Cadence, a comparison is made between Balun LNA with and without degeneration of the CS stage.

Another technique used in this design is the forward body biasing (FBB) which reduced the Vth of the transistors [18]. FBB is when the body is connected to a DC supply (or gate) instead of source or ground. In the case of CG, the body is directly connected to the gate, as no AC signal is present on the gate. However, for the CS, the body cannot be connected to the gate as an AC signal is present, the body is connect to its own biasing voltage or before the biasing resistor.

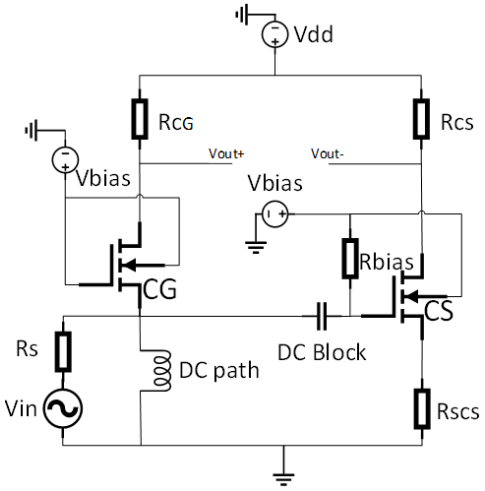

FIGURE 2. Balun LNA using NMOS UMC180nm with CS degeneration.

TABLE 1. Balun LNA circuit parameters.

Element	Description	CG	CS
N_L18W500_18_RF	Width (um)	120	315
N_L18W500_18_RF	Length (nm)	180	180
N_L18W500_18_RF	gm (mS)	20	35
MIMCAPM_RF	DC block (pF)	-	10
RNNPO_RF	RD (Ohm)	200	150
Resistor (Cadence library)	Degeneration (Ohms)	-	8
Vbias with R_{SCS}	Biasing (mV)	510	550
Vbias without R_{SCS}	Biasing (mV)	510	510
RNNPO_RF	Biasing (Ohm)	-	2K
Current	ID (mA)	2.07	4.67

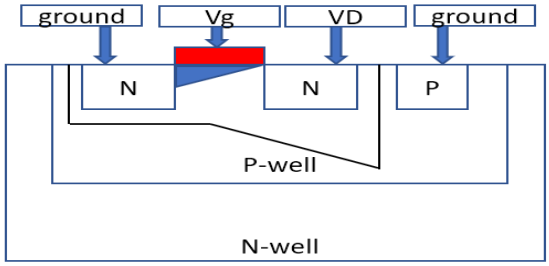

FIGURE 3. NMOS cross section area with body grounded.

Fig (3) and Fig (4) shows a cross sectional diagram of the NMOS device. It illustrates the body connection and its effect on the depletion region, the depletion region around the drain has a huge impact on the channel and adding FBB increases the concentration of the electrons, therefore reducing the Vth needed to drive the NMOS.

$$\overline{I_{nCG}}: \quad \overline{I_{nCG}}\left[R_{CG}+R_{CG}g_{mCG}R_s-\frac{1}{g_{mCG}} * \frac{g_{mCS}R_{CS}}{1+g_{mCS}R_{SCS}}-\frac{g_{mCS}R_{CS}R_s}{1+g_{mCS}R_{SCS}}\right] \quad (33)$$

$$\overline{I_{nCS}}: \quad \overline{I_{nCS}}\left[\frac{1+g_{mCS}R_{SCS}}{g_{mCS}} * g_{mCG}R_{CG}+\frac{(1+g_{mCS}R_{SCS})}{g_{mCS}} * g_{mCG}^2R_{CG}R_s\right.$$
$$\left.-R_{CS}-R_{CS}g_{mCG}R_s\right] \quad (34)$$

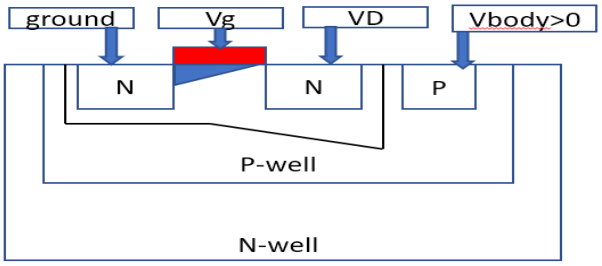

FIGURE 4. NMOS cross section area with body biased.

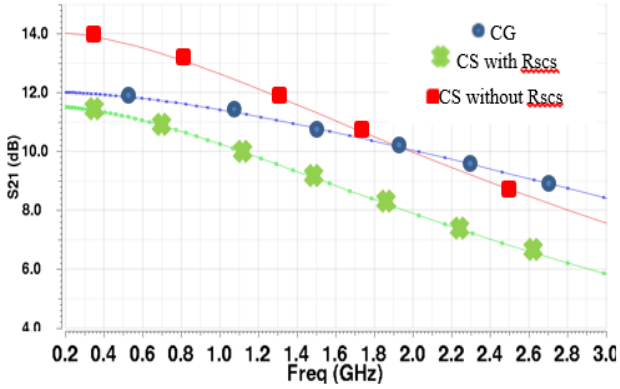

FIGURE 5. Gain vs frequency of CG, CS and CS with degeneration.

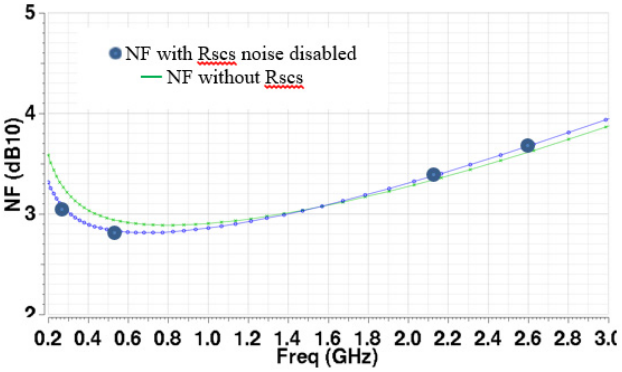

FIGURE 6. LNA NF with CS degeneration resistor (resistors noise is disabled) and without CS degeneration.

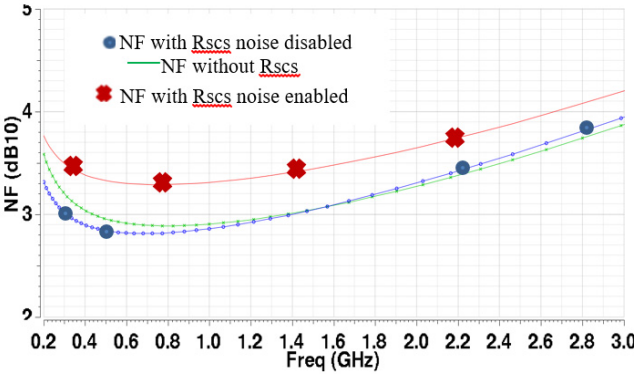

FIGURE 7. LNA NF with CS degeneration resistor (resistors noise is disabled), CS degeneration resistor (resistors noise is enabled) and without CS degeneration.

In Fig (5), CG gain, CS without degeneration and CS with degeneration gain are plotted. Before the addition of R_{SCS}, the gain unbalance at the low frequencies is 2 dB. After the addition of the R_{SCS}, gain unbalance is reduced to 0.4db. The noise was disable in the R_{SCS} to check the validity of whether the thermal noise can be canceled if balanced with a degeneration source.

Fig (6) shows the NF comparison between the LNA with and without R_{SCS}. A drop in NF after balancing indicates that R_{SCS} can be used to balance and cancel the transistors thermal noise. This means another degree of freedom has been added to the design of the Balun LNA.

Without R_{SCS}, the unbalance created by the CS stage is more than the unbalance created than with R_{SCS}. A higher unbalanced gain output is present without R_{SCS}, which result in a higher NF at low frequencies,shown in Fig (5) and Fig (6). However, with the addition of R_{SCS}, the unbalanced was reduced resulting in a decrease in NF, but at higher frequencies where the unbalance was increased due to R_{SCS} the noise of the LNA is increased. Fig (7) shown NF of the LNA when the noise of R_{SCS} was enabled, the overall NF of the LNA is increased by an average of 0.4 due the resistors own thermal noise contribution. However, the linearity increases due to adding the degeneration source must be accounted for.

VII. LINEARITY TEST

Sweeping input power from −20dbm to 0 dBm.

Fig (8) and Fig (9) are the P1dB compression points at 900MHz. Fig (8) is the LNA with Rscs and Fig (9) is the LNA without Rscs. An increase in linearity is noticed with the addition of Rscs of around 1.4dBm.

$$\overline{Vin^2_{LNA}} = \frac{\gamma g_{mCG}\left(R_{CG} + R_{CG}g_{mCG}R_s - \frac{1}{g_{mCG}} * \frac{g_{mCS}R_{CS}}{1+g_{mCS}R_{SCS}} - \frac{g_{mCS}R_{CS}R_s}{1+g_{mCS}R_{SCS}}\right)^2}{R_s * A^2_{vLNA}} + \frac{\gamma g_{mCS}\left(\frac{g_{mCG}R_{CG}(1+g_{mCS}R_{SCS})}{g_{mCS}} + \frac{(1+g_{mCS}R_{SCS})g^2_{mCG}R_{CG}R_s}{g_{mCS}} - R_{CS} - R_{CS}g_{mCG}R_s\right)^2}{R_s * A^2_{vLNA}} \quad (37)$$

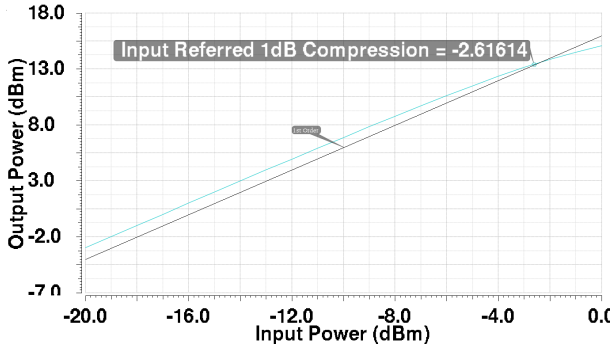

FIGURE 8. P1dB with CS degeneration @900MHz is −2.6.

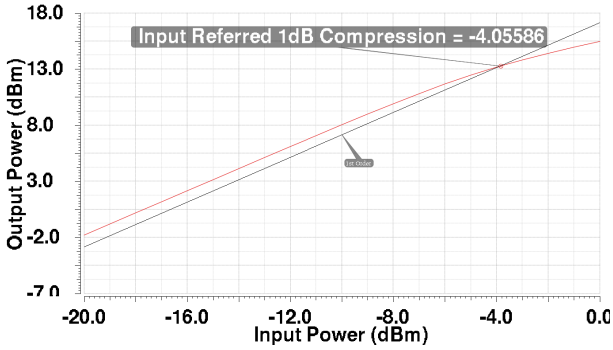

FIGURE 9. P1dB without CS degeneration @900MHz is −4.

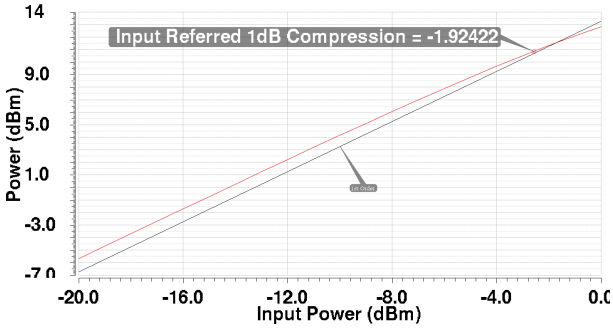

FIGURE 10. P1dB with CS degeneration @2.4GHz is −1.9.

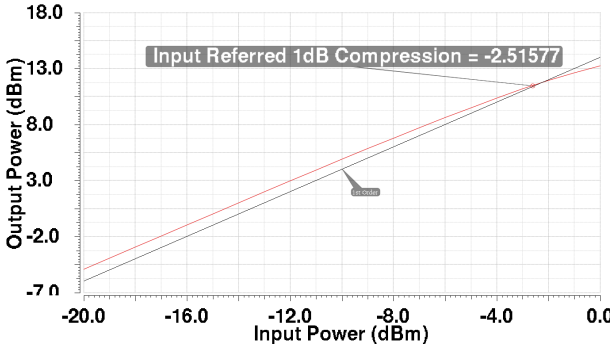

FIGURE 11. P1dB without CS degeneration @2.4GHz is −2.5.

Fig (10) and Fig (11) are the P1dB compression points at 2.4GHz. Fig (10) is the LNA with Rscs and Fig (11) is the LNA without Rscs. An increase in linearity is noticed with the addition of Rscs of around 0.6dBm.

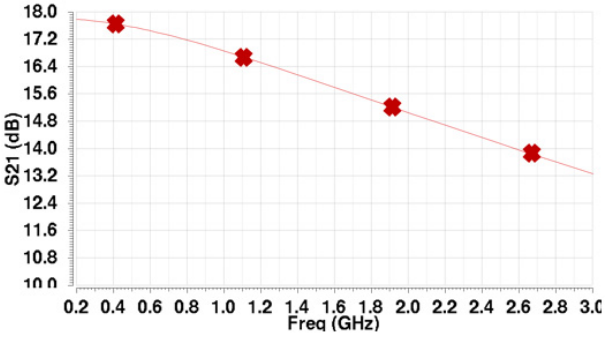

FIGURE 12. Total LNA gain vs frequency with CS degeneration. BW=200M-2.1GHz.

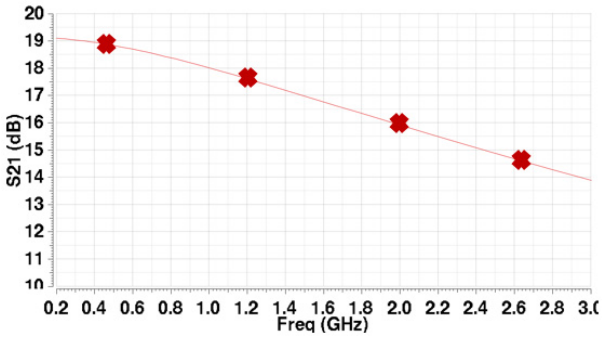

FIGURE 13. Total LNA gain vs frequency without CS degeneration, BW=200M-1.9GHz.

Fig (12) is the LNA total voltage gain with R_{SCS}, and Fig (13) is the total gain without R_{SCS}. The LNA did lose 1.2dB in gain, but the bandwidth is increased by 200MHz.

In addition to the condition set in [1], another balancing condition for the Balun LNA can be added by using a degeneration resistor. If the Balun LNA is balanced, equation (37) will give you zero, meaning R_{SCS} does not need to be added.

If $g_{mCS} > g_{mCG}$ by a factor of "n", $R_{CS} > R_{CG}$ by a factor of "m" and the CG satisfies the matching condition $R_S = 1/g_{mCG}$ the following set of balancing condition can be derived:

$$g_{mCS} = n g_{mCG} \tag{39}$$

$$R_{CS} = m R_{CG} \tag{40}$$

$$R_S = \frac{1}{g_{mCG}} \tag{41}$$

Substituting (39), (40), (41) into (36):

$$R_{scs} = \frac{mn g_{mCG} R_{CG} - g_{mCG} R_{CG}}{n g_{mCG} g_{mCG} R_{CG}}$$

$$\Rightarrow R_{scs} = \frac{mn - 1}{n g_{mCG}}$$

$$\Rightarrow R_{scs} = \frac{mn - 1}{n} * R_S \tag{42}$$

Equation (42) expresses R_{scs} as a function of the unbalance multiplier factor "n" and "m" in terms of R_S.

TABLE 2. Comparison with state of the art LNAS.

Ref	Tech (nm)	Band (GHz)	Gain (dB)	NF (dB)	IIP3 (dBm)	Power (mW)	Balun
[9]* 2004	250	0.2-2.0	10-14	<2.4	0	35	NO
[10]* 2006	90	0.5-8.2	22-25	<2.6	-4/-16	42	NO
[11] 2006	90	0.8-6	18-20	<3.5	>-3.5	12.5	YES
[1]* 2008	65	0.2-5.2	13-15.6	<3.5	>0	14	YES
[12] 2009	90	0.1-1.9	20.6	<2.7	10.8	9.6	YES
[3] 2010	130	0.2-3.8	11.2	<2.8	-2.7	1.9	YES
[7] 2013	130	6-9	22	<3.2	-	5.5	YES
[13] * 2016	180	0.01-1.7	19.7	<2.8	1.13	25.2	YES
[15]* 2019	65	0.05-1	24-30	2.3-3.3	>-4	19.8	YES
[14] 2019	180	0.21-1.1	18.5-15.5	2.8-3.8	-13.4	5.58	YES
This work Without Rscs	180	0.2-1.9	19-16	<3.6	<8	12	YES
This work With Rscs	180	0.2-2.1	17.8-14.8	<3.8	<7.9	12	YES

References denoted by "" in Table II are measured results other results are simulated.*

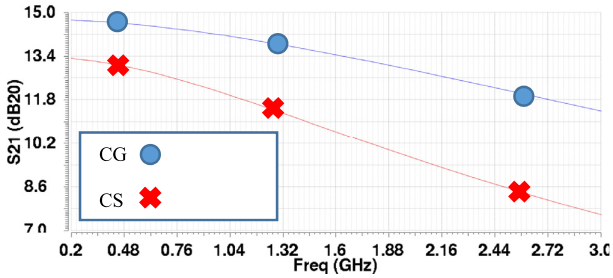

FIGURE 14. CS and CG gain at fast corner at −40°C.

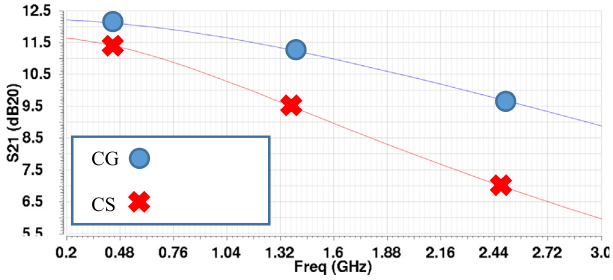

FIGURE 15. CS and CG gain at typical corner at 27°C.

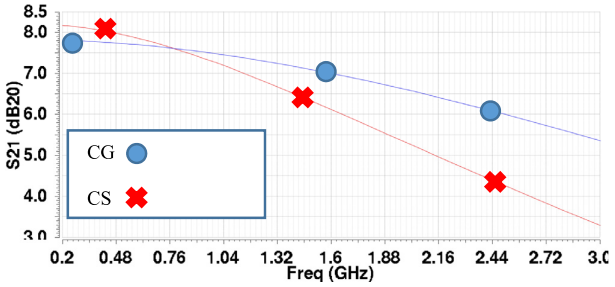

FIGURE 16. CS and CG gain at slow corner at 125°C.

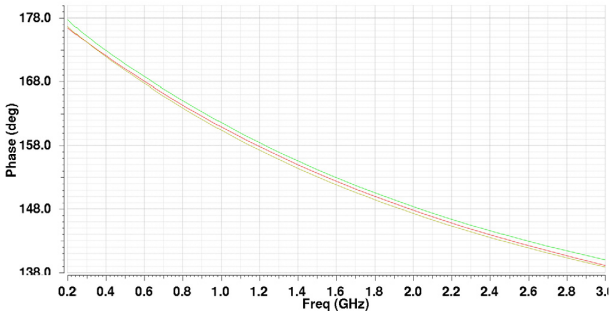

FIGURE 17. The LNA output phase at different corners, since the difference between fast and slow corner phases is only 2°, the output phase of the LNA at the three corners appear to be identical.

VIII. PROCESS-VOLTAGE-TEMPERATURE VARIATION

The PVT (fast, typical and slow corner at −40,27 and 125°C) for the LNA with degeneration resistor are simulated in this section, where the voltage gain, voltage gain unbalance and output phase are plotted. An ideal DC block was used at the input when simulating the AC analysis, and the biasing was not changed.

From Fig (14-16), the CG has suffered the most variation due to the PVT, where the gain at 200MHz at the corners is 15.6dB at fast corners and 7.7dB at slow corner (7.9dB drop from fast to slow), while the CS is 13.4dB at fast corners and 8.2dB at slow corner (5.2dB drop from fast to slow). In Fig (17) the different phase of the output of the LNA is plotted for the three corners, a phase difference of 2° is present between fast and slow corners, hence why Fig (17) appears to have one plot.

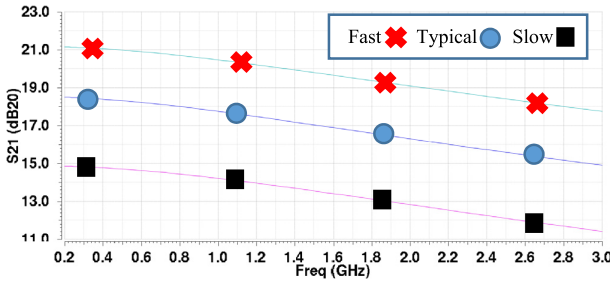

FIGURE 18. Total LNA gain at fast (−40°C), typical (27°C) and slow (125°C).

IX. CONCLUSION

Balun is a differential pair, therefore the thermal noise is expected to cancel if the LNA is designed properly. Step by step analysis of the noise was given in this paper where it was shown that the condition for balancing will cancel the thermal noise of the Balun transistors and not only the CG stage. If the unbalance of the output gain is created due to the CS stage having higher gain than the CG stage, the addition of a degeneration resistor to the CS to balance the output is presented. The degeneration resistor impact on the thermal noise cancelation was derived and simulated to see if the reduction of the gain unbalance with a degeneration resistor can reduce the transistors thermal noise(or cancel it) without changing the transconductance gm or the drain resistors Rd. A new set of conditions revolving around CS degeneration were derived. Thermal noise cancelation is due to the gain being out of phase while the thermal noise is in phase. Since the Balun LNA takes the difference in the output, the thermal noise is subtracted.

ACKNOWLEDGMENT

This paper represents the opinion of the author(s) and does not mean to represent the position or opinion of the American University of Sharjah.

REFERENCES

[1] S. C. Blaakmeer, E. A. M. Klumperink, D. M. W. Leenaerts, and B. Nauta, "Wideband balun-LNA with simultaneous output balancing, noise-canceling and distortion-canceling," *IEEE J. Solid-State Circuits*, vol. 43, no. 6, pp. 1341–1350, Jun. 2008.

[2] W. Zhuo, X. Li, S. Shekhar, S. H. K. Embabi, J. P. de Gyvez, D. J. Allstot, and E. Sanchez-Sinencio, "A capacitor cross-coupled common-gate low-noise amplifier," *IEEE Trans. Circuits Syst. II, Exp. Briefs*, vol. 52, no. 12, pp. 875–879, Dec. 2005.

[3] I. Bastos, B. L. Oliveira, J. Goes, and M. Silva, "MOSFET-only wideband LNA with noise cancelling and gain optimization," in *Proc. 17th MIXDES*, Warsaw, Poland, 2010, pp. 306–311.

[4] L. Albasha, "Design and measurement of an integrated wideband radio frequency low-noise amplifier for terrestrial digital television applications," *Int. J. Electron.*, vol. 97, no. 5, pp. 587–604, May 2010.

[5] J. Tao, X. Fan, X. Chen, and Y. Zhao, "A differential balun-LNA for multistandard receivers in 0.13 μm BiCMOS," in *Proc. IEEE Int. Conf. Automat., Electron. Electr. Eng. (AUTEEE)*, Shenyang, China, Nov. 2018, pp. 150–153.

[6] J. Sturm, S. Popuri, and X. Xiang, "CMOS noise canceling balun LNA with tunable bandpass from 4.6 GHz to 5.8 GHz," in *Proc. 21st IEEE Int. Conf. Electron., Circuits Syst. (ICECS)*, Marseille, France, Dec. 2014, pp. 84–87.

[7] Z. Li, L. Sun, and L. Huang, "A high-gain low-power balun-LNA for 6–9 GHz UWB system," in *Proc. Asia–Pacific Microw. Conf. Proc. (APMC)*, Seoul, South Korea, Nov. 2013, pp. 264–266.

[8] P. Qin and Q. Xue, "A CMOS active balun-LNA with imbalance correction and noise cancelling," in *Proc. IEEE Int. Workshop Electromagn., Appl. Student Innov. Competition (iWEM)*, Nanjing, China, May 2016, pp. 1–3.

[9] F. Bruccoleri, E. A. M. Klumperink, and B. Nauta, "Wide-band CMOS low-noise amplifier exploiting thermal noise canceling," *IEEE J. Solid-State Circuits*, vol. 39, no. 2, pp. 275–282, Feb. 2004.

[10] J.-H.-C. Zhan and S. S. Taylor, "A 5 GHz resistive-feedback CMOS LNA for low-cost multi-standard applications," in *IEEE Int. Solid-State Circuits Conf. (ISSCC) Dig. Tech. Papers*, San Francisco, CA, USA, Feb. 2006, pp. 721–730.

[11] R. Bagheri, A. Mirzaei, S. Chehrazi, M. E. Heidari, M. Lee, M. Mikhemar, W. Tang, and A. A. Abidi, "An 800-MHz–6-GHz software-defined wireless receiver in 90-nm CMOS," *IEEE J. Solid-State Circuits*, vol. 41, no. 12, pp. 2860–2876, Dec. 2006.

[12] P. Mak and R. Martins, "Design of an ESD-protected ultra-wideband LNA in nanoscale CMOS for full-band mobile TV tuners," *IEEE Trans. Circuits Syst. I, Reg. Papers*, vol. 56, no. 5, pp. 933–942, May 2009.

[13] L. Liu, Z. Lu, K. Zhang, Z. Ren, A. Hu, and X. Zou, "Wideband balun-LNA exploiting noise cancellation and gm' compensation technique," *Electron. Lett.*, vol. 52, no. 8, pp. 673–674, Apr. 2016.

[14] S. Tiwari and J. Mukherjee, "An inductorless noise cancelling wideband balun LNA with dual shunt feedback and current reuse," in *Proc. IEEE 62nd Int. Midwest Symp. Circuits Syst. (MWSCAS)*, Dallas, TX, USA, Aug. 2019, pp. 432–435.

[15] S. Kim and K. Kwon, "A 50-MHz–1-GHz 2.3-dB NF noise-cancelling balun-LNA employing a modified current-bleeding technique and balanced loads," *IEEE Trans. Circuits Syst. I, Reg. Papers*, vol. 66, no. 2, pp. 546–554, Feb. 2019.

[16] Q. Abubaker and L. Albasha, "On the noise analysis of the balun LNA," in *Proc. IEEE Asia–Pacific Conf. Appl. Electromagn. (APACE)*, Melacca, Malaysia, Nov. 2019, pp. 70–73.

[17] B. Razavi, *Design of Analog CMOS Integrated Circuits*. Singapore: McGraw-Hill, 2001, pp. 47–80.

[18] M. Parvizi, K. Allidina, and M. N. El-Gamal, "Short channel output conductance enhancement through forward body biasing to realize a 0.5 V 250 μW 0.6-4.2 GHz current-reuse CMOS LNA," *IEEE J. Solid-State Circuits*, vol. 51, no. 3, pp. 574–586, Mar. 2016.

QUSAI M. ABUBAKER was born in Irbid, Jordan, in 1995. He received the B.S. degree (Hons.) in electrical and electronics engineering from the University of Sharjah, Sharjah, UAE, in 2017. He is currently pursuing the master's degree with the American University of Sharjah. From 2017 to 2019, he was a Graduate Teaching Assistant with the American University of Sharjah. His research interests include low powered applications, LNA, and harvesters.

LUTFI ALBASHA (Senior Member, IEEE) joined Sony Corporation after graduation and worked on commercial RFIC chip products. He then joined Filtronic Semiconductors as a Senior Principal Engineer and created the integrated circuits design team. The team supported the company foundry design enablement for mass production and taped-out its first range of commercial chips. He returned to Sony as a Lead Principal Engineer and worked on highly integrated CMOS transceivers for cellular and TV applications. He joined the American University of Sharjah and is currently a Professor with the Department of Electrical Engineering. His current areas of research interest include energy harvesting, low-power implantable devices, and integrated radar transceivers. He received several outstanding Recognition Awards from Sony Corporation, the IET, the IEEE, and the University of Leeds. He is an Associate Editor of *IET Microwaves, Antenna and Propagation* journal and served as President of the UAE Chapter of IEEE Solid-State Circuits Society for Three years.